Shock Waves in Space Environments

Devrie S. Intriligator, Thomas Detman, James Intriligator, Christine Gloeckler, Wei Sun, W. David Miller, William R. Webber, and Murray Dryer

Citation: AIP Conference Proceedings **1183**, 167 (2009); doi: 10.1063/1.3266773
View online: http://dx.doi.org/10.1063/1.3266773
View Table of Contents:
http://scitation.aip.org/content/aip/proceeding/aipcp/1183?ver=pdfcov
Published by the AIP Publishing

Shock Waves in Space Environments

Devrie S. Intriligator[1], Thomas Detman[1], James Intriligator[1,2], Christine Gloeckler[3], Wei Sun[1,4], W. David Miller[1], William R. Webber[5], and Murray Dryer[1,6]

1. Carmel Research Center, P.O. Box 1732, Santa Monica, CA 90406, USA
2. Bangor University, Bangor, Wales, LL572AS, UK
3. Department of Atmospheric, Oceanic, and Space Sciences, University of Michigan, Ann Arbor, MI 48109, USA;
4. Geophysical Institute, University of Alaska, Fairbanks, AK 99775, USA
5. New Mexico State University, Las Cruces, NM 88005, USA
6. NOAA/Space Weather Prediction Center, 325 Broadway, Boulder, CO 80305, USA

Abstract. We present results on two topics: a) The three-dimensional (3D) Hybrid Heliospheric Modeling System with Pickup Ions (HHMS-PI) simulations of shock waves and initial comparisons with ACE and Ulysses data for the Halloween 2003 solar events, including the Ulysses SWICS pickup proton densities; and b) Our analyses of Voyager 2 (V2) data near the termination shock (TS). Previously, we used our time-dependent 3D Hybrid Heliospheric Modeling System (HHMS) for magnetohydrodynamic (MHD) simulations of transient events originating on the Sun. We now have added the physics of "pickup" proton processes to these models. Interstellar neutral hydrogen flows into the heliosphere and becomes ionized by photoionization and by charge exchange with solar wind protons. These "pickup" protons cause a slowing and heating of the solar wind flow in the outer heliosphere. Both HHMS-PI and HHMS use *continuous* solar inputs to simulate processes that originate at the Sun. Our V2 analyses identified some elevated readings in the plasma subsystem (PLS) data. It is tempting to interpret these at face value as detections of high energy ions (HEIs) which may interact with the bulk convective plasma through a two stream instability giving rise to the observed enhanced signals in the plasma wave subsystem (PWS).
Keywords: solar variability effects, solar wind plasma & fields, interplanetary magnetic fields, interplanetary propagation, heliosphere interstellar medium interaction, shocks, pickup ions
PACS: 96.60.Q.-, 96.50sh, 96.50-e, 96.50.Bh, 96.50Xy,96.50Ya,96.60

INTRODUCTION

The 3D simulations starting at the Sun [1-9] can address fundamental questions of solar transient propagation in the 3D time-dependent global heliosphere. The 3D MHD HHMS has a well-established history [1-4] and has shown successful modeling of the propagation of solar transients. The next section of this paper is an update of our recent inclusion of pickup protons [10,11] in our *continuous* 3D MHD modeling [1-9] of the background solar wind and of transient events originating at the Sun that give rise to shock waves in the interplanetary medium. We compare HHMS-PI simulation results with data. The HHMS and HHMS-PI and their *continuous* solar inputs actually capture shocks, corotating interactions regions (CIRs), stream-stream interactions, merged interaction regions, rarefaction regions, etc. These models also study the propagation of solar phenomena starting from the Sun, which is essential for understanding the time-dependent 3D global heliosphere. While these models are not perfect, their predictions provide important insights into the propagation of the solar wind throughout the heliosphere and beyond. We present the correlation coefficients (r_c) between the model

CP1183, *Shock Waves in Space and Astrophysical Environments*
edited by X. Ao, R. H .Burrows, and G. P. Zank

results and the associated observations for each of our parameter runs. Both the higher and lower r_e are useful since they help to reveal the significant underlying physical mechanisms in the interplanetary medium.

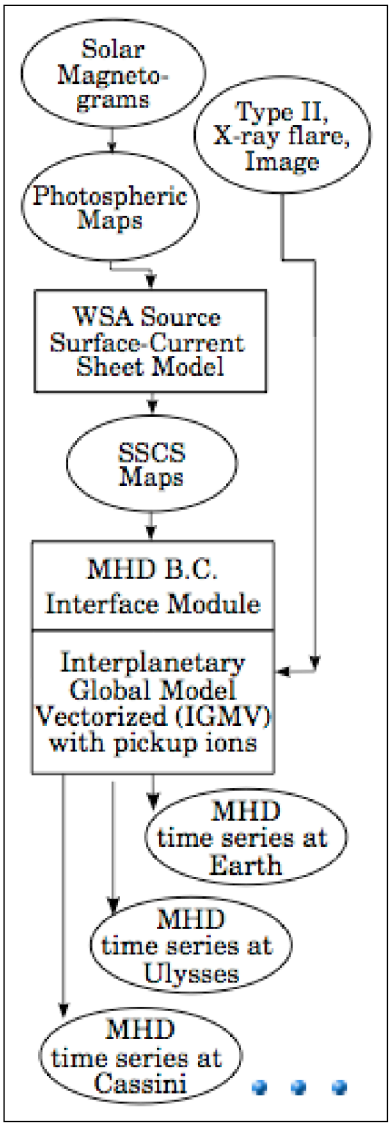

FIGURE 1. Schematic showing the two tracks in the full 3D MHD HHMS-PI. *Continuous* inputs of solar parameters are input into both the background solar wind track on the left and the solar transient track on the right.

Last year, we showed [8] that even performing a 3D simulation originating at the Sun in isolation, that is, not in the context of the preceding and following ambient solar wind and CIRs as well as solar events, can lead to erroneous conclusions concerning the event's interplanetary propagation and the asymmetries associated with the event's propagation throughout the heliosphere. This year we also discuss this topic since we find that even for the powerful and numerous Halloween 2003 solar events, the shocks and other phenomena associated with their interplanetary propagation are greatly influenced by the background solar wind and CIRs.

V2 was the first spacecraft to measure in detail the heliospheric TS. In August 2007 the TS crossed over V2 on Day 242 (August 30) during a data gap when the spacecraft was not being tracked. The next day when V2 was in the heliosheath the PWS detected enhanced plasma wave activity in the 31 and 56 kHz channels [12, 13]. Gurnett et al. [12] labeled this enhanced activity "Event A" and suggested it was associated with a TS crossing. They were informed [13] that the V2 PLS [14] and magnetometer [15] data did not indicate a TS crossing at the time of Event A. To investigate the origin of Event A we analyzed the PLS data. We found that there were elevated readings on the sunward-facing B-Cup [16] during this time, which - if taken at face value - imply that high energy ions (HEIs) were measured during Event A. In the second section below we present some of our results on the V2 HEI detections and discuss some physical mechanisms that may be responsible for the enhanced PWS Event A activity.

3D MHD HHMS-PI RESULTS

The schematic of HHMS-PI is shown in Figure 1. The 3D MHD solar wind model in HHMS PI (and HHMS) has a *continuously* changing lower boundary condition (at 0.1 AU) that is driven

indirectly by the Wang-Sheeley-Arge (WSA) source surface current-sheet model. The WSA model is a steady state model of the solar corona. We used full (Carrington) rotation maps, generated by the NOAA Space Weather Prediction Center, available at <ftp://helios.sec.noaa.gov/pub/lmayer/WSA/full_fits_ss_maps/MWO/>. The interval between these maps is the Carrington rotation period, 27.2753 days. However, since the input to the WSA model consists of daily solar magnetograms over a solar rotation combined into a global magnetic map of the photosphere, the resulting source surface (SS) maps have an effective update interval of about a day. We interpolate in time between two maps to update the boundary condition for each time step of our model.

For our purpose, the ouput is a global magnetic map at a height of five solar radii (5 R_S). Typically, SS maps are generated daily. HHMS uses a sequence of SS maps to create a *time-continuous* quasi-steady background lower boundary condition and resulting solar wind. This process (on the left in Fig. 1) gives a global, pre-event, inhomogeneous, background solar wind plasma and interplanetary magnetic field (IMF). The model captures the buildup of CIRs. Transient events (on the right in Fig.1) are superimposed on the background. Our treatment of pickup ions follows that of Usmanov and Goldstein (2006) [17]. Briefly, we treat pickup ions (protons, henceforth PI) as a separate fluid with its own density and temperature, but the pickup ions and solar wind share a common velocity. Details of the coupling are the same as Usmanov and Goldstein [17].

We recently completed our initial inclusion of pickup protons into the time dependent 3D full MHD HHMS-PI with an outer boundary at 5.5 AU. We show the initial comparisons of the modeled HHMS-PI results with ACE data at 1 AU and with Ulysses data at ~ 5 AU for the Halloween 2003 events which occurred in October/November 2003. During this time ACE and Ulysses were separated [5] by ~ 120 degrees in longitude and ~ 5 degrees in latitude.

Table 1 summarizes the solar events from October 19 to November 20, 2003 associated with the Halloween 2003 events in the same format as our previous tables [5] and indicates the input data for the HHMS-PI transient tract (on the right in Fig. 1). We note that many groups performed simulations on these events [18-21]. Once these data are input into HHMS-PI nothing is adjusted or changed and the model runs from the Sun out in 3D going past the Earth and ACE, out to Ulysses. Eventually HHMS-PI will run to Cassini and Voyager 1 and 2 in the outer heliosphere and beyond. The input data in Table 1 are the final inputs that were used in HHMS-PI to produce the agreements between HHMS-PI and the ACE and Ulysses data shown in Figures 2 and 3, respectively. The inputs in Table 1 were obtained by an iterative shock input "tuning" process. Our strategy was to begin with the originally published [5] Fearless Forecast (FF) shock strength, location, and duration parameters, run the model and then estimate simulated shock arrival times and compare them with those observed. To obtain agreement between simulated and observed shock times of arrival at ACE it was only necessary to adjust the input shock speed. As described in [1], we simply multiplied the old shock input speed by the ratio of observed shock travel time to the old simulated shock travel time; in the absence of other changes, three or four iterations were usually sufficient.

For a period of strong activity, such as Halloween 2003, finding the correct pairing of solar (FF) events with observed shock arrivals at ACE is a non-trivial problem. Our first few tuning runs led to some changes from our original pairing. In the second phase of our strategy, we extended the model to 5.5 AU and compared simulated with observed

shock arrivals at Ulysses. At this point, with two spacecraft, our tuning process was more complicated, and the pairing of observed shocks at Ulysses with solar FF events was more ambiguous, due mainly to the increased distance and travel time. Adjusting shock inputs to match "target" arrival times at two different spacecraft required changing more than one of the inputs. To keep it as simple as possible, we limited our tuning to three of our five shock input parameters, shock speed (Vs), shock longitude (lon), and shock input radius (rad); the remaining two parameters, shock latitude (lat) and shock duration (tau), were kept fixed at the values given in the original FF. These parameters describe a perturbation to our background solar wind lower boundary condition at 0.1 AU (21.5 R_S). The shock perturbation was applied to a circular area on the grid boundary; centered at (lat, lon) having radius (rad) on the grid boundary. Since the grid boundary is spherical, technically rad is like a great circle distance, except that it is given in degrees. In other words, from the center of the sun (r = 0), the perturbation radius subtends the angle rad. Each shock has a peak speed in a direction given by (lat, lon); the shock speed decreases across the shock front as one moves away from the direction of the peak. At some angle away from the peak speed, determined by the Vs and rad parameters, and propagation distance the shock speed reduces to that of a fast mode wave plus the local flow speed. Thus a single (peak) shock speed can be used to match propagation times at two locations, but only within reasonable limits.

Running the extended model with shock inputs tuned for ACE gave disappointing results at Ulysses. Even after several "bi-tuning" runs, we could not reproduce the high solar wind speeds seen at Ulysses around Day 320. To obtain the results in Figures 2 and 3, we added the event listed as FF# 520.2 in the first column of Table 1. Analysis of Ulysses data by de Koning [22] indicated the occurrence of a strong solar event beyond the visible disk of the Sun on 11/07 at 15:54 UT. A longitude of W120, and latitude of S18 is consistent with this event coming from the same active region (10486) that produced FF520, FF517, and/or FF514. When we added this event to our shock inputs and tuned it to arrive at Day 318.984, we also got a very good match with a reverse shock at Ulysses near Day 320 that produced the highest speeds at Ulysses in the study interval.

Figure 2 presents the comparisons between the HHMS-PI simulations and the ACE data from Day 290-340, 2007. There is a 0.93 correlation coefficient (r_c) between the simulated and measured solar wind speeds for the entire 50-day interval shown in Fig. 2. The high r_c is a result of parameter tuning. We have two kinds of tuning: we tune model parameters to improve the background mode agreement with ACE data, and we tune shock input parameters to get the desired shock arrival times at ACE.

The comparison between the simulated and observed IMF parameter in the second panel in Fig. 2 yields a r_c of 0.54 for the entire 50-day interval shown. The model generally agrees better with the magnitude of the background IMF, but it does not capture as well the IMF excursions of the variations. We are continuing to analyze these differences in the hopes of improving the r_c. This is an example of how our delving into the reasons for the lower r_c may lead to a more sophisticated understanding of the physical mechanisms at work. The third panel in Fig. 2 shows the simulated and measured solar wind proton temperature. For the entire 50-day interval shown the r_c is 0.78. It is evident that there is generally good agreement between the proton temperature

Table 1. October 19 - November 20, 2003 solar events and HHMS-PI inputs*

FF#	Date	Time	Day	Lat	Lon	Rad	Vs(km/s)	Tau
0507	10-19	1650	292.701	N05	E56	102	519.6	1.33
0508	10-21	0347	294.158	S10	E90	100	517	0.67
0509	10-22	0938	295.401	S02	E22	100	781.5	3.00
0510	10-23	0827	296.352	S21	E88	108	1276	1.50
0511	10-25	0415	298.177	S15	E43	120	530	2.00
0512	10-26	0617	299.262	S18	E43	120	574.1	3.00
0513	10-26	1735	299.733	N05	W32.6	70.2	1027	3.50
0514	10-28	1102	301.460	S16	E08	120	1951	3.00
0515	10-29	2044	302.864	S14	W1	123	1612.4	1.50
0516	11-01	2234	305.940	S10	W61	120	820.9	1.00
0517	11-02	1714	306.718	S14	W82.53	158	1791.42	1.00
0518	11-03	0124	307.058	N10	W85	100	725	1.75
0519	11-03	0956	307.414	N08	W77	120	1131.3	1.50
0520	11-04	1943	308.822	S19	W78.84	102	1580.7	1.50
0520.2	11-07	1554	311.663	S18	W120	100	1642.7	2.00
0521	11-11	1335	315.566	S03	W88.77	93.7	807	3.00
0522	11-13	0924	317.392	N01	E90	101	710.5	3.00
0523	11-17	0917	321.387	S01	E33	100	547	2.00
0524	11-18	0747	322.324	N00	E18	221.1	918.4	3.00
0525	11-20	0747	324.324	N01	W14	104.9	997.9	0.75

*FF#: real-time "fearless forecast" events. Date & Time: start time of metric Type II. Rad: width of shock (degrees). Vs (km/s): shock speed input at the Sun from real-time radio & halo/partial halo CME plane-of-sky speed estimates. Tau (hrs): coronal shocks piston driving time above flare site.

simulation and the data except just after Day 295 and Day 305 and – to a lesser extent – after Day 335 when the data show a strong cooling of the protons. Here again our further analyses of these differences between the simulation and the data may provide physical insights into the processes responsible for the observations – in this case the cooling of the solar wind. The bottom panel in Fig. 2 shows the modeled and measured solar wind proton density. The r_c is 0.43. While this value is low, comparison between the simulation results and the data shows that generally the model captures the data trends: it simulates the big density increases ~ Day 298, after Day 300, ~ Day 305, ~Day 309, after Day 310, ~ Day 315, at Day 319, and ~ Day 325. However, for example, even though the model correctly simulates density decreases ~Day 300, 315, 325, and 330 it over estimates these densities. Future analyses should yield a deeper understanding of the processes at work and their interactions during these complex events.

Figure 3 compares some of the HHMS-PI simulation results with Ulysses data obtained at ~ 5 AU and at a large longitudinal separation (> 90 degrees) from Earth [5]. The top panel displays the simulated and SWOOPS measured solar wind speeds. As discussed above, we tuned to get the r_c of 0.92. We could not get a good match until we added the FF520.2 event. This event arrived on Day 318.984 and the highest speeds, seen on Day 320, are associated with a reverse shock that originated with FF517. We believe

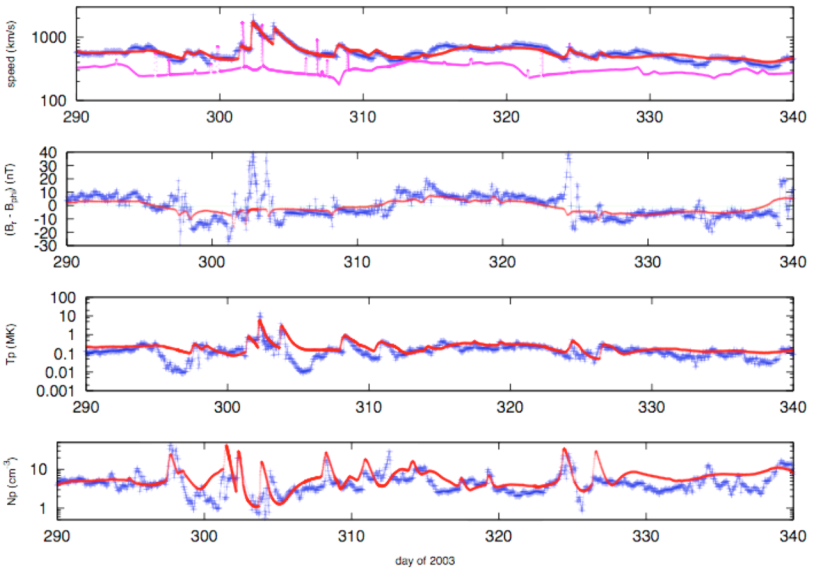

FIGURE 2. Comparison of HHMS-PI results with ACE data from Day 290 to 340, 2003. In each of the panels the HHMS-PI simulations are the smooth red line and the ACE data are shown with the blue individual + points. The top panel shows the HHMS-PI simulated speeds and the ACE solar wind speed (km/s), with the simulated speed overlying the data points for most of this 50 day interval including for the multiple shock arrivals between ~ Day 297 – 310. For the entire interval, we tuned to obtain a correlation coefficient r_c of 0.93 between the simulated speeds and the speed data. The light magneta line below the 1 AU speeds shows the speeds at 0.1 AU, the initial location of the solar wind speeds in the model. The second panel shows the IMF parameter (Br-Bphi) in nT. The third panel shows the solar wind proton temperature Tp (MK), and the bottom panel displays the solar wind proton density Np (cm^{-3}). See text.

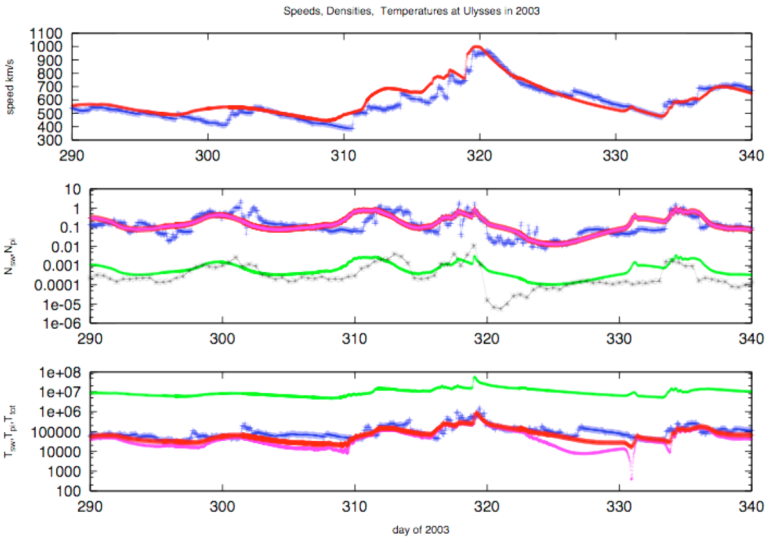

FIGURE 3. Comparison of HHMS-PI results with Ulysses SWOOPS and SWICS data. See text.

it is the interaction between these two events that gives the good agreement with observed speeds, FF520.2 arrives at Day 318.984 and the reverse shock from FF517 arrives on Day 320 (just after interacting with FF520.2). Errors in speed near Day 300 and 310 are quite noticeable; these are entirely background mode errors (i.e., from the left tract in Fig. 1). In the second panel in Fig. 3 both the measured SWOOPS solar wind proton densities and the measured SWICS [10] pickup proton densities are compared with the HHMS-PI simulation results. In the upper set of curves the blue data points show the SWOOPS proton densities and the red line shows the HHMS-PI simulation of the solar wind proton density. In the second set of curves the black data points display the SWICS measured pickup proton densities and the green line the HHMS-PI simulation for the pickup proton densities. The r_c for the solar wind proton density comparison is 0.53 and for the pickup proton density it is 0.50. There is good agreement between the HHMS- PI simulations and the data trends, but for ~ Day 310, 320, and 330-340 the simulation overestimates the densities. We are pleased with the agreement between the SWICS measured background pickup proton densities and the HHMS-PI predictions. This is our initial prediction with HHMS-PI for pickup protons and given the complexity of the Halloween 2003 events, this agreement is an indication of the value of HHMS-PI and it robustness. The bottom panel in Fig. 3 shows the HHMS-PI simulations for the temperatures: solar wind proton (red), the pickup proton (green), the total solar wind proton and pickup proton (magenta), and the SWOOPS measured solar wind proton (blue points). The r_c is 0.78 between the simulated and solar wind proton temperature data. At this time there are no SWICS pickup proton temperatures available for comparison.

This initial application of HHMS-PI to the complex Halloween 2003 events shows we were able to tune to obtain excellent agreements between the simulated speeds and those measured at ACE and Ulysses, the shock arrival times, and their associated speed jumps. While the correlation coefficients for the other simulated parameters and the data are not as high, they indicate a good initial basis for further studies. We are optimistic that future work with HHMS-PI will provide many important insights into the global 3D heliosphere, its response to solar transients, and the role of pickup protons.

ANALYSES OF V2 DATA NEAR THE TERMINATION SHOCK

Figure 4 shows the V2 PWS data obtained near the TS in 2007. The enhanced PWS signals labeled "Event A" are intriquing since Gurnett et al. [12] suggested that they could be associated with a V2 TS crossing but the PLS [14] and magnetometer [15] data did not appear to support this association. However, using PLS data provided to us by John Richardson (the PLS Principal Investigator) we have found elevated readings in the PLS sunward-facing B-Cup [16] at energy per charge (E/Q) step 12 in L-mode during Event A which we interpret as a second plasma component of high energy ions (HEIs) in the plasma. The PLS E/Q spectra in Figure 5 were detected during Event A and appear to show the two plasma populations: the bulk convective plasma with its proton speed of <~200 km/s and the HEI plasma with a proton speed of ~600 km/s. While these elevated readings at E/Q step 12 could be a PLS instrument anomaly not to be taken at face value, or the result of a change in the plasma/spacecraft environment, we suggest that they may be associated with a HEI plasma. If the HEIs are protons they have a speed of ~ 600 km/s

(independent of the bulk convective plasma speed), a density of 10^{-4} cm^{-3}, and a thermal speed of 10 km/s (Richardson, private communication, 2009). The interaction of the HEIs with the bulk convective plasma could give rise to a two stream plasma instability - consistent with that modeled in Gurnett et al. [12] associated with the ramp of the third V2 TS crossing – producing the enhanced PWS signals observed in Event A in Fig. 4.

One test of the validity of these HEI detections is that during a "control" interval of Days 1-90, 2007, there were no elevated readings or HEI detections on the B-Cup. It is tempting to associate the elevated HEI readings in Fig. 5 with TS reflected protons similar to the pickup protons observed near the Mars bow shock by Dubinin et al. [23]. They found that the speed of the pickup ions reflected by the Mars bow shock did not track the speed of the bulk flow plasma and that the speed of the reflected ions was higher than expected. Both of these characteristics are similar to those of the TS HEIs shown in Fig. 5.

Richardson has informed us that the higher energy channels of the V2 PLS suffered radiation damage in Jupiter's magnetosphere. Since that time noise has persisted in the upper energy channels of the L mode, adding current to some cups and subtracting current from others. This noise is not constant but undergoes random shifts that are not understood. Recently current has been added to the A- and C-Cups and subtracted from B-Cup. The PLS team does not know if these shifts are related to the plasma environment, changes in the spacecraft, or changes in the instrument electronics. Thus, if the PLS is operating nominally and the elevated readings can be taken at face value, the currents on the B-Cup shown in Fig. 5 are likely *underestimates* of the actual plasma currents present near the V2 TS. As the B-Cup elevated readings in Fig. 5 are all well above the instrument's minimum possible readings, it is tempting to consider them real and significant. If the elevated readings can be taken at face value, whether they are indicative of the detection of HEIs or of a plasma/spacecraft environmental effect or of

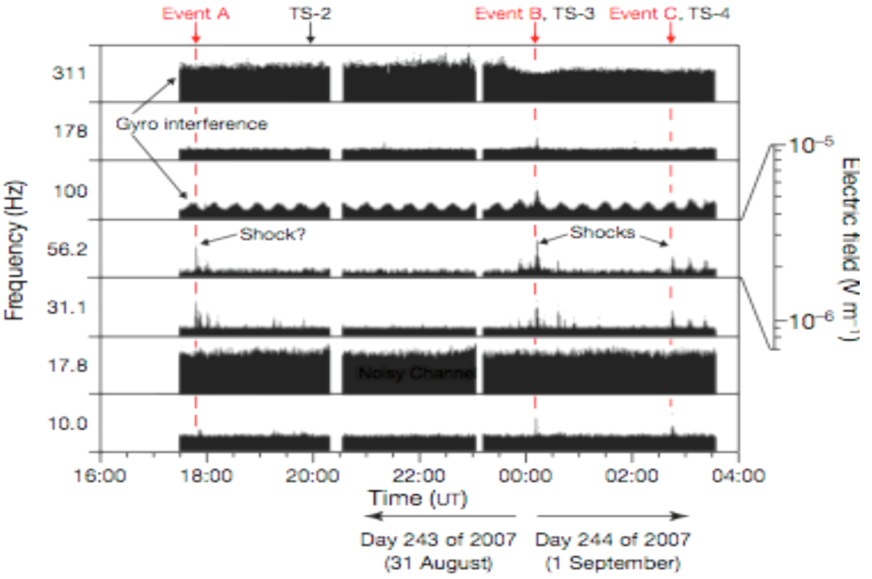

FIGURE 4. Voyager 2 PWS data [12] of the enhanced plasma wave signals associated with Event A and the termination shock crossings in 2007.

changes in the plasma/spacecraft environment, they may offer additional insights into the physical mechanisms and processes taking place when V2 is near the TS or they may provide insights into the changes in the plasma/spacecraft environment which in turn may help reveal the physical processes taking place when V2 is near the TS. As these are the only in-situ plasma observations available near the TS, with no more likely for decades, if the elevated readings detected by the V2 PLS are not HEIs, and are associated with plasma/spacecraft environment changes or effects, further study of them may provide greater understanding of the physical environment and/or processes in this region. Similarly, if the elevated plasma detections cannot be taken at face value due to an instrument anomaly, further analyses may reveal the physical cause of this problem.

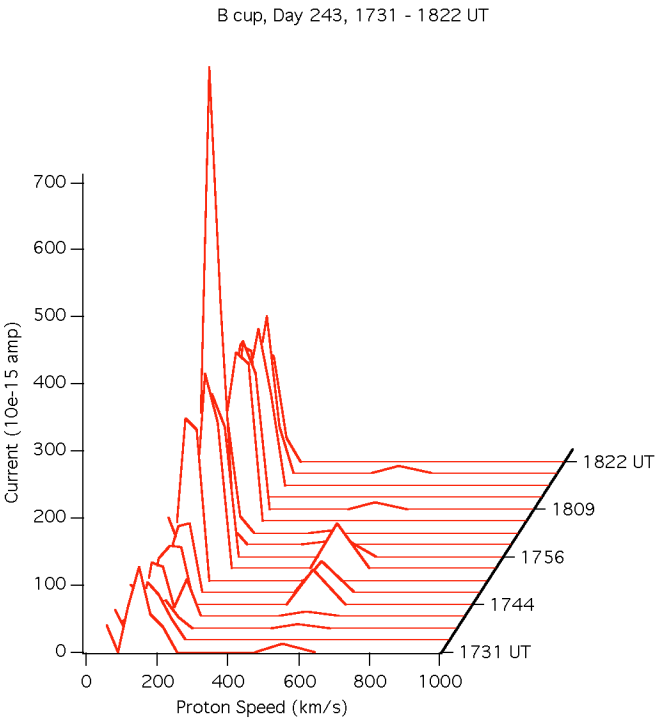

FIGURE 5. Voyager 2 E/Q spectra of PLS ion detections on the sunward-facing B-Cup in L-Mode scans [16] as a function of average proton speed (v_p) near Event A in the PWS data (Fig. 4). Start times of some E/Q spectra are shown. The bulk plasma v_p is < 200 km/s. The HEIs are not present in all spectra. We associate them with the elevated readings at E/Q step 12 ~ 1610 volts, i.e., v_p of ~ 554 km/s.

SUMMARY

Shock waves are an important aspect of space environments. We summarized the initial results for the Halloween 2003 solar events using HHMS-PI which incorporated pickup ions into the 3D MHD HHMS. These 3D models with *continuous* solar inputs are essential for the interpretation of in-situ data at diverse heliospheric locations. We tuned

the HHMS-PI solar input parameters of shock location, speed, and width to achieve excellent agreement (e.g., $r_c > 0.9$) between the HHMS-PI simulations of solar wind speed and the ACE and Ulysses measured speeds showing shock arrival times, the speed jumps associated with the shock arrivals, etc. The HHMS-PI modeled pickup proton density and temperature were presented and compared with available Ulysses SWICS data. With regard to the V2 PLS data near the TS, if the elevated readings can be taken at face value, they indicate the presence of HEIs. It is tempting to associate the enhanced plasma wave signals during Event A as being due to a two-stream instability from the interaction of the beam of HEIs with the bulk convective plasma flow.

ACKNOWLEDGMENTS

We thank the Voyager, ACE, and Ulysses teams and the NSSDC for the plasma, IMF, and plasma wave data, and trajectory information. This work was supported in part by NASA grant NNX08AE40G with Carmel Research Center. The work by DSI and JI also was supported in part by Carmel Research Center. We thank the reviewer for a number of constructive suggestions.

REFERENCES

1. T. R. Detman, C.N. Arge, V. Pizzo, Z. Smith, M. Dryer, and C.D. Fry, *J. Geophys. Res., 111*, A07102, doi:10.1029/2005JA0111430, 2006.
2. D. S. Intriligator, T. Detman, W. Sun, C. Fry, M. Dryer, C. Deehr, Z. Smith, and J. Intriligator, Solar Wind 11, ESA Publ. SP-592, pp 343-346, 2005.
3. D. S. Intriligator, T. Detman, W. Sun, C.Fry, M. Dryer, C. Deehr, Z. Smith, J. Intriligator, SHINE, 2005.
4. D. S. Intriligator, T. Detman, M. Dryer, C. Fry, W. Sun, C. Deehr, and J. Intriligator, The Physics of Collisionless Shocks, (Ed., G. Li), Amer. Inst. of Phys. Conf. Proc. 781, 304, 2005.
5. D. S. Intriligator, W. Sun, M. Dryer, C. Fry, C. Deehr, and J. Intriligator, *J. Geophys. Res.,* doi:10.1029/2004JA010939, 2005.
6. D. S. Intriligator, M. Dryer, W. Sun, C.D. Fry, C. Deehr, and J. Intriligator, Physics of the Outer Heliosphere, (Eds., V. Florinski, N. Pogorelov, and G. Zank) AIP 719, 2004.
7. D. S. Intriligator, A. Rees, and T. Horbury, W. Sun, T. Detman, M. Dryer, C. Deehr, and J. Intriligator, Turbulence and Nonlinear Processes in Astrophysical Plasmas, (Eds., D. Shaikh, G. Zank), Amer. Inst. of Phys. Conf. Proc. 932, 167, 2007.
8. D. S. Intriligator, W. Sun, A. Rees, T. Horbury, W.R. Webber, C. Deehr, T. Detman, M. Dryer, and J. Intriligator, Particle Acceleration and Transport in the Heliosphere and Beyond (Eds. G. Li, Q. Hu, O. Verkhoglyadova, G. Zank, R. Lin, and J. Luhmann) AIP 1039, 375-383, 2008.
9. D. S. Intriligator, W. Sun, T. Detman, M. Dryer, C. Fry, C. Deehr, and J. Intriligator, Physics of the Inner Heliosheath, (Ed., J. Heerikhuisen), Amer. Inst. of Phys. Conf. Proc. 858, 64, 2006.
10. Gloeckler, G., J. Geiss, E. Roelof, L. A. Fisk, F. Ipavich, K. Ogilvie, L.J. Lanzerotti, R. von Steiger, and B. Wilken, Acceleration of interstellar pickup ions in the disturbed solar wind observed on Ulysses, *J. Geophys. Res., 99*, 17637-17647, 1994.
11. Intriligator, D.S., G.L. Siscoe, and W.D. Miller, Interstellar Pickup H+ Ions at 8.3 AU: Pioneer 10 Plasma and Magnetic Field Analyses, *Geophys. Res. Lett., 23(16)*, 2181-2184, 1996.
12. Gurnett, D.A., W. S. Kurth, L.F. Burlaga, M. H. Acuna, N.F. Ness, J.D. Richardson, and N. Omidi, Electrostatic waves observed at and near the solar wind termination shock by Voyager 2, in Particle Acceleration and Transport in the Heliosphere and Beyond, 7th Annual International Astrophysics Conference, AIP 1039, page 335 - 342, 2008.
13. Gurnett, D., and W. Kurth, *Nature 07023, 454*, doi:10.10.38, 2008.
14. Richardson, J. D., J. Kasper, C. Wang, J. Belcher, & A. Lazarus, Cool heliosheath plasma and deceleration of the upstream solar wind at the termination shock, *Nature* 07024, *454*, doi:10.10.38/ p.63 – 66, July, 2008.

15. Burlaga, L.F., N. Ness, M. Acuna, R. Lepping, J. Connerney, & J. Richardson, Magnetic fields at the solar wind termination shock, *Nature 07029, 454*, doi:10.10.38/ p.75 – 77, July, 2008.
16. Bridge, H.S., J.W. Belcher, R. Butler, A.J. Lazarus, A.M. Mavretic, J. D. Sullivan, G.L. Siscoe, and V.M. Vasyliunas, The plasma experiment on the 1977 Voyager mission, *Space Sci. Rev., 21*, 259-287, 1977.
17. Usmanov, A.V. and M. Goldstein, A three-dimensional MHD solar wind model with pickup protons, *J. Geophys.Res., 111,* A07101,doi:10.1029/2005JA011533,2006.
18. Dryer, M. Z. Smith, C. Fry, W. Sun, C.S. Deehr, and S.-I. Akasofu, Real-Time predictions of interplanetary shock arrivals at L1 during the "Halloween 2003" spoch, *Space Weather, 2*, S09001, doi:10.1029/2004SW000087, 2004.
19. Krall, J., V. Yurchyshyn, S. Slinkler, R. Skoug, J. Chen, Flux rope model of the 2003 Oct. 28 – 30 coronal mass ejection and interplanetary coronal mass ejections, *Ap. J., 643*, 541, 2006.
20. Lui, Y., and K. Hayashi, The 2003 Oct.-Nov. fast halo coronal mass ejections and the large scale magnetic field structures, *Ap. J., 640*, 1135, 2006.
21. Manchester,W., A. Vourlidas, G. Toth, N. Lugaz, I. Roussev, D. De Zeeuw, M. Opher, T. Gombosi, D.De Zeeuw, Three-dimensional MHD simulation of the 2003 Oct. 28 coronal mass ejection: Comparison with LASCO coronograph obsrvations, *Ap. J, 684*, 1448, 2008.
22. de Koning C. A., J. T. Steinberg, J. T. Gosling, D. B. Reisenfeld, R. M. Skoug, O. C. St. Cyr, M. L. Malayeri, A. Balogh, A. Rees, D. J. McComas (2005), An unusually fast interplanetary coronal mass ejection observed by Ulysses at 5 AU on 15 November 2003, *J. Geophys. Res., 110*, A01102, doi:10.1029/2004JA010645.
23. Dubinin, E.. M. Fraenz, J. Woch, S. Barabash, R. Lundin, and M. Yamauchi, Hydrogen exosphere at Mars: Pickup protons and their acceleration at the bow shock, *Geophys. Res. Lett., 33*. L22103, doi:10.1029/2006GL027799, 2006.